IL NUOVO CIMENTO Vol. 36 C, N. 6 Novembre-Dicembre 2013
DOI 10.1393/ncc/i2014-11640-7

Colloquia: LaThuile13

Invariant mass distribution of jet pairs produced in association with a W boson at CDF

M. Trovato on behalf of the CDF Collaboration

Scuola Normale Superiore - Pisa, Italy and
Fermi National Accelerator Laboratory - Batavia, Il, USA

ricevuto il 20 Giugno 2013; approvato l'1 Luglio 2013

Summary. — We present a study of the invariant mass spectra of jets produced in association with a W boson decaying into a lepton and a neutrino. Events of this signature are critical to studies of vector boson pair production, top-quark physics, Higgs boson physics, and searches for beyond the standard model particles. We present a search for high-mass resonances decaying into jets, and find no significant excess above the standard model background prediction.

PACS 14.70.Dj – Gluons.
PACS 14.70.Fm – W Bosons.
PACS 14.80.-j – Hypothetical particles.
PACS 14.80.Tt – Technicolor.

1. – Introduction

At hadron colliders the production of jet pairs in association with vector bosons offers measurements of fundamental standard model (SM) fundamental parameters and tests of theoretical predictions. Several beyond-SM (BSM) scenarios also predict significant deviations from the SM in these signatures [1-3]. In a previous publication, the CDF collaboration reported a disagreement between data and the SM prediction using a data sample corresponding to $4.3\,\mathrm{fb}^{-1}$ of integrated luminosity [4]. Assuming an excess of events over the background prediction appearing as a narrow Gaussian distribution, the statistical significance of the reported disagreement was 3.2 standard deviations. In this current document, we report an update of the previous analysis using the full CDF Run II data set (about twice as much as the previous analysis). In the course of these studies, new calibrations of the detector response and instrumental backgrounds were performed, yielding a better agreement with the standard model predictions. No significant excess above the SM predictions is observed.

2. – Event selection

Missing transverse energy ($\not\!\!E_T$) is defined as the opposite of the vector sum of all calorimeter tower energy depositions projected on the transverse plane. It is used as a measure of the sum of the transverse momenta of the particles that escape detection, most notably neutrinos. The corrected energies are used for jets in the vector sum defining $\not\!\!E_T$. When muons are identified, the muon momentum, as measured from the tracking system, is used to compute $\not\!\!E_T$.

Muon and electron candidates used in this analysis are identified during data taking by the CDF trigger system, by requiring the transverse energy $E_T > 18\,\text{GeV}$ for central electrons (TCE) and the transverse momentum $p_T > 18\,\text{GeV}/c$ for muons (CMUP, CMX). Offline, we require the transverse energy (or momentum) to be more than 20 GeV (GeV/c) and the $|\eta|$ to be less than 1.1 (1). TCE, CMUP, and CMX are identified if they pass a number of requirements which are listed in [5]. An example of those requirements for the electrons is the ratio between the hadronic and electromagnetic energy, which has to be lower than $0.055 + 0.00045 \cdot E$, E being the electron energy.

We select events with one and only one electron with $E_T > 20\,\text{GeV}$ or muon with $p_T > 20\,\text{GeV}/c$, large transverse missing energy ($\not\!\!E_T > 25\,\text{GeV}$), and exactly two jets with $E_T > 30\,\text{GeV}$ and $|\eta| < 2.4$. In order to reject multijet backgrounds we impose the following cuts: the transverse mass of the lepton and $\not\!\!E_T$ system $m_T > 30\,\text{GeV}$, the azimuthal angle between the most energetic jet and $\not\!\!E_T$, $\Delta\phi(\not\!\!E_T, j1) > 0.4$, the difference in pseudorapidity between the two jets, $|\Delta\eta(j_1, j_2)| < 2.5$, and the transverse momentum of the dijet system $p_T^{jj} > 40\,\text{GeV}/c$.

3. – JES modeling

The jets used in this analysis have their energies, as measured by the calorimeter, corrected for a number of effects that distort the true jet energy. These effects include consistency across $|\eta|$ and time, contributions from multiple $p\overline{p}$ interactions per beam crossing (pileup), the non-linear response of the calorimeter. The jet energy scale (JES) corrections applied are described in detail in [6].

These energy corrections, however, do not distinguish between the response to gluon and quark jets. The largest energy corrections, which correct the energy scale of calorimeter jets to better match that of particle jets and the initial parton energies, are derived using PYTHIA [7] dijet Monte Carlo simulations. Differences in the response to gluon and quark jets between MC and data may lead to differences in the measured energies of these objects, which are not covered by the previously assigned systematic uncertainties on the JES.

We derive a correction for the response to quark and gluon jets in data and simulated events by using two independent samples of jets with different quark fractions, which are obtained from the MC. In these samples the balancing information of jets against objects of known momentum is used. We use events where a jet balances with a high-E_T photon, which are rich in quark jets, and utilize the $Z \to \ell^+\ell^-+$ jet events, which are more rich in gluon jets. Both datasets correspond to an integrated luminosity of $8.9\,\text{pb}^{-1}$. We construct the balance of the jet with these reference objects:

$$K_{Z/\gamma} = (E_T^{jet}/p_T^{Z/\gamma}) - 1. \tag{1}$$

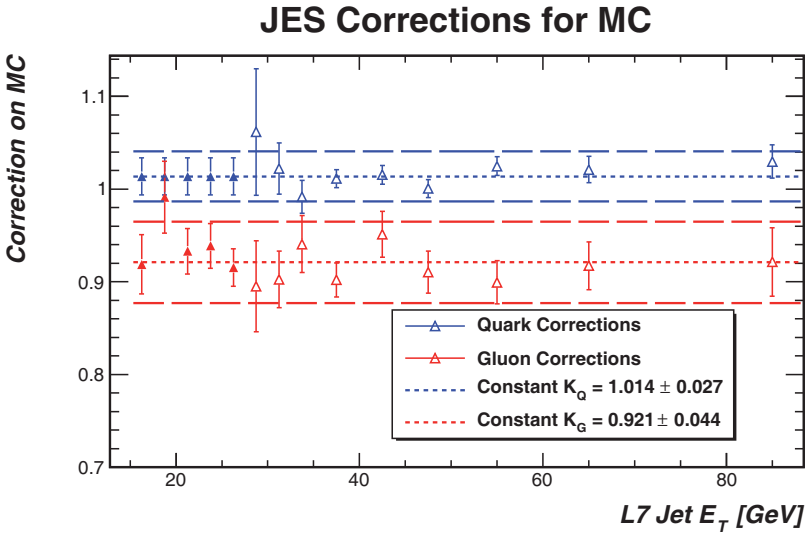

Fig. 1. – The derived correction for simulated quark jets (blue) and gluon jets (red) as a function of $E_T{}^{\text{jet}}$. The open triangles represent corrections derived using both γ-jet and Z-jet balancing samples, while the filled triangles represent the assumed flat correction for quarks and the corresponding correction for gluons calculated from the Z-jet balancing sample alone. The error bars shown are statistical uncertainties only. The short dashed lines are the fits of the correction to a constant across jet E_T, and the long dashed lines represent the total systematic uncertainty bands on that constant correction, further described in text.

For well-measured jets, $K_{z/\gamma} = 0$. Rather than deriving full and separate JES corrections for quark and gluon jets in data and simulation, we compare the balance in data and simulation, and derive an additional correction to be applied to simulated jets, based upon whether these jets are matched to quarks or gluons. Those corrections are shown in fig. 1. Due to the photon trigger used to select the γ-jet balancing sample, we do not have reliable balancing information for jets below 27.5 GeV in that sample, therefore limiting the full range over which we may derive corrections. Since we are interested in jets down to energies around 20 GeV, we extrapolate to lower jet energies the quark jet energy correction derived for jets with $E_T \geq 27.5$ GeV, and use the Z-jet balancing sample to extract a gluon correction assuming this extrapolated quark correction.

As both the quark and gluon corrections appear flat in jet energy for jets with $E_T \geq 15$ GeV, we fit them to a constant. We find that to better match the data, quark jet energies in MC should be increased by $(1.4 \pm 2.7)\%$, while gluon jet energies should be decreased by $(7.9 \pm 4.4)\%$.

The considered sources of uncertainty for the aforementioned corrections are summarized in table I. Because the corrections shift the energy response in simulation to better match data, the quark jet and gluon jet energy correction uncertainties are anti-correlated: if the quark jet energy correction goes up, the gluon jet energy correction must go down in order to compensate for that shift, and viceversa. The uncertainties are similar in magnitude to the default CDF jet energy scale uncertainties [6].

TABLE I. – *Summary of the additional jet energy corrections applied to MC jets, and the uncertainty on those corrections. F^Q, N_{vert} refer, respectively, to the quark fractions and the number of vertices in the γ or Z samples. The uncertainties for the quark jet and gluon jet energy corrections are anticorrelated, as they must work in concert to match the balancing distributions in data.*

Jet Energy Correction		Quark jets 1.014	Gluon jets 0.921
Uncertainty	Fit/Statistics	0.020	0.025
	$F_Q^{Z-\text{jet}}$	0.006	0.021
	$F_Q^{\gamma-\text{jet}}$	0.018	0.027
	Low E_T extrapolation		0.004
	N_{vert}	0.002	0.012
	Total Uncertainty	± 0.027	∓ 0.044

4. – Multijet background modeling

Three-jet events can be misidentified as signal when one of the jets fakes the lepton. This mismeasurement or other mismeasurements in the calorimeter may result in relatively large missing transverse energy. In muon events, a number of studies show that the multijet background is negligible ($< 0.5\%$), while in electron events is about 8%. In this section we will concentrate on describing the multijet estimation and the systematic analysis for events with electrons. Same methods are applied to muon events, although, since the multijet contribution to muon events is much smaller, the effect of this background in the final analysis is much less important.

To model the multijet background we use side-band data, which is selected exactly in the same way as described in sect. **2**, except for some of the electron identification cuts which are inverted (*e.g.*: ratio between the hadronic and electromagnetic energy). The objects identified with those inverted cuts are named "non-electrons". This ensures that the sample we use as multijet model is orthogonal to our signal sample and at the same time kinematically similar. To test the validity of our model we exploit a third (control) region, which has the same selection cuts as the one described in sect. **2**, except that we require events to have either $\not\!\!E_T < 20\,\text{GeV}$ or $m_T < 30\,\text{GeV}$. Such a region was chosen to be orthogonal to the signal region and to be enriched of the multi-jets background ($\sim$ 85% of the total) such that possible deficiencies in our model would be enhanced.

When looking at the electron E_T distribution in the control region, we notice that the non-electron model is unable to predict the data (fig. 2). The observed deficit at $E_T \lesssim 35\,\text{GeV}$ is due to trigger biasing the non-electron distribution. Infact, since the trigger cuts on the cluster electromagnetic energy only, some of the non-electron events with low electromagnetic energy fraction will not be able to pass the trigger requirements. Such an effect is not present for the electron candidates since their energy is almost purely electromagnetic. In order to remove the trigger bias, we reweight non-electron events such that the predicted electron spectrum agrees with the data. This reweighting is done in the control region and the same weights applied to non-electrons are used in the signal region. Other minor corrections for the non-electron model are reported in [8].

In order to test the effect of these corrections we check the modeling of an important

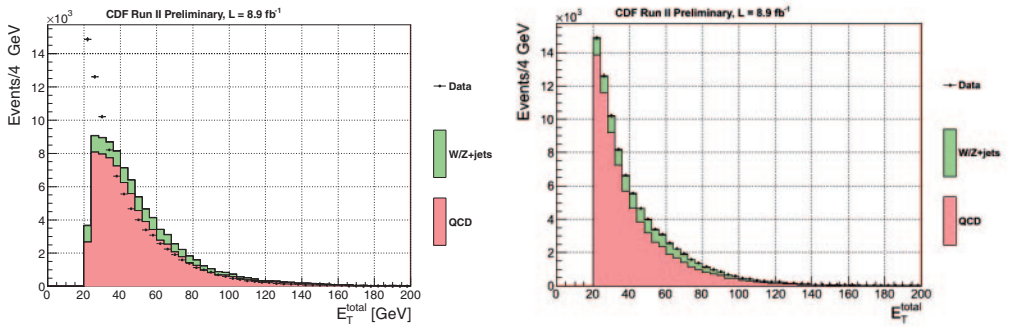

Fig. 2. – The electron energy distribution in the control region as observed in the data and as predicted by the non-electron–based model before (left) and after (right) the corrections.

kinematic distribution for this analysis: the P_T of the 2-jet system. Figure 3 shows this quantity before and after applying our correction in the control region defined above. Same level of significant improvement can be seen in other kinematical variables as well.

5. – Invariant mass spectrum

In order to model the data we perform a fit in dijet invariant mass by maximizing an appropriately defined binned likelihood function. The multi-jets backgrounds shapes for the electron and muon samples are obtained respectively from the non-electron (sect. **4**) and the not-isolated muon samples. Rates are obtained by fitting the $\not\!\!E_T$ in the data [8]. The origin of the shapes in the fit and the rate constraints, which are implemented in the likelihood function, are summarized in table II.

The fit is preliminary performed without considering the correction to the multijet background model (sect. **4**), and to the jet energy scale (sect. **3**). Similar to [4], aside from SM contributions we allow in the fit a Gaussian component centred at 145 GeV/c^2 with a width of 14.3 GeV/c^2 (fig. 4). Assuming an acceptance identical to the one for a 140 GeV/c^2 Higgs produced in association with a W boson, the cross section determined

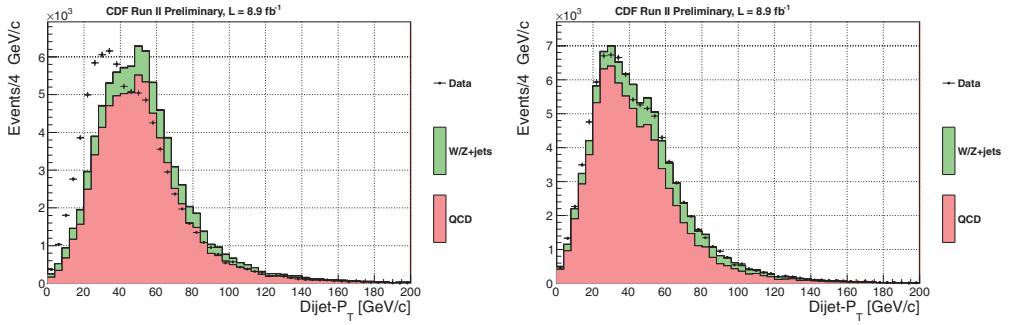

Fig. 3. – P_T of the 2-jet system before (left) and after (right) applying the corrections described in text for the multijet enriched selection.

TABLE II. – *MC generators used to derive the dijet invariant mass shapes of each indicated process. The rate constraints in the maximum-likelihood fit are either obtained from the theory or from the data.*

Process	Shapes	Rate constraint
Diboson	PYTHIA	Theory (±6%)
$t\bar{t}$	PYTHIA	Measured cross section [9]
single-top	MadEvent+PYTHIA	Theory (±6%)
W/Z+jets	ALPGEN+PYTHIA	None
Multi-jet background	from data	from data

would be 2.4±0.6 pb. A similar discrepancy between data and prediction can be observed in both electrons and muons (fig. 5). Nonetheless, it is clear that a simple Gaussian does not describe well the excess observed in data.

We now perform the same aforementioned fit after including the aforementioned corrections described in sect. **3** and sect. **4**. We will first look at the effect of the correction due to different response to quarks and gluons as described in sect. **3**. The two samples (electrons and muons) are shown in fig. 6. Good agreement between data and the prediction is seen in the muon sample. For the electron sample the agreement is better, but still poor. However, after applying the correction to the multijet background, the electron sample shows a good agreement (fig. 7).

The result of the simultaneous fit in the electron and muon samples is shown in fig. 8. In this case, the data is consistent with no excess around 145 GeV/c^2. Therefore, we establish at a 95% CL $\sigma^{WX} < 0.9$ pb upper limit on the cross section of a possible resonance X produced in association with a W boson, decaying into two jets, and with 145 GeV/c^2 mass.

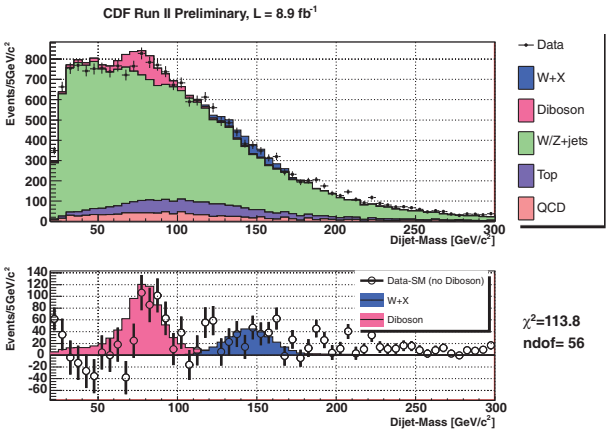

Fig. 4. – Fit to the dijet invariant mass distribution similar to [4]. The corrections described in text have not been applied. Bottom figure shows data with all backgrounds (except the diboson contribution) subtracted.

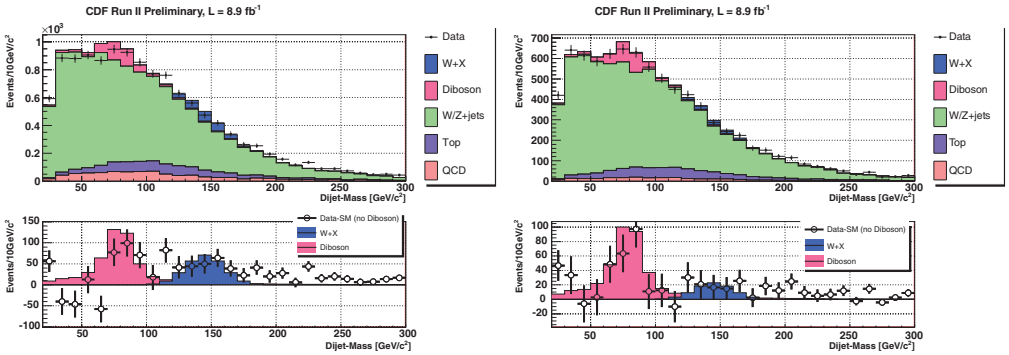

Fig. 5. – Fit to the dijet invariant mass distribution similar to [4]. The corrections described in text have not been applied. Bottom figures shows data with all backgrounds (except the diboson contribution) subtracted. On the left we show the invariant mass distribution in electron events and on the right the invariant mass distribution in muon events.

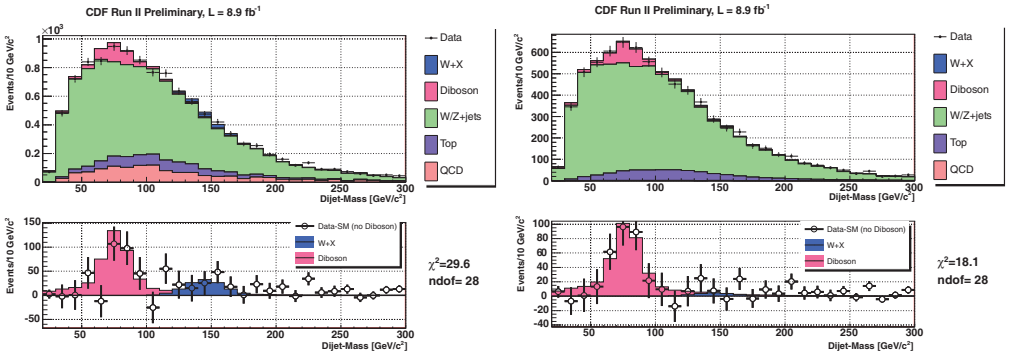

Fig. 6. – Fit to the dijet invariant mass distribution for electrons (left) and muons (right). The jet energy scale corrections for MC described in the text have been applied. Bottom figure shows data with all backgrounds (except the diboson contribution) subtracted.

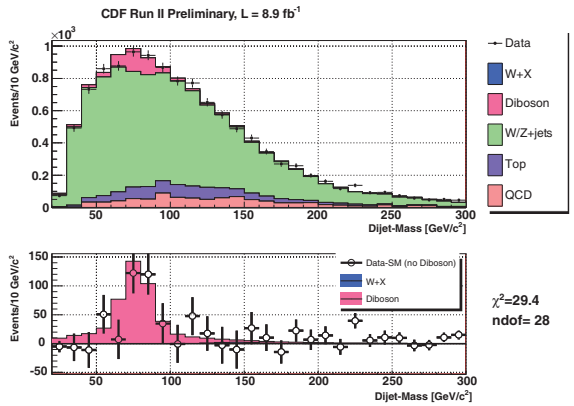

Fig. 7. – Fit to the dijet invariant mass distribution in the electron sample. All corrections described in text have been applied. Bottom figure shows data with all backgrounds (except the diboson contribution) subtracted.

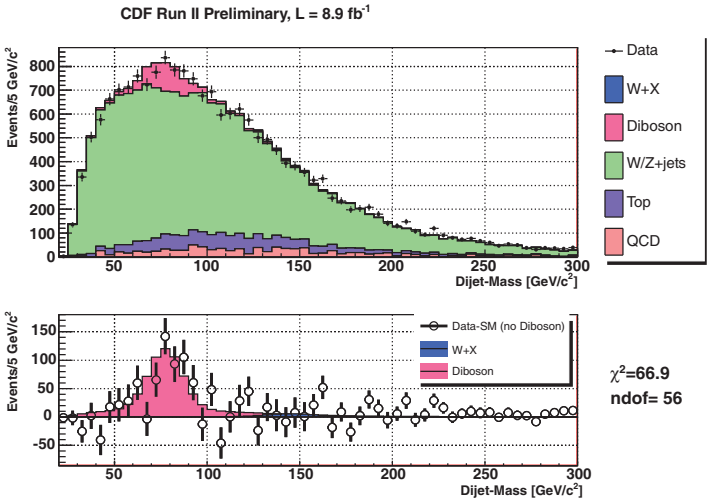

Fig. 8. – Fit to the dijet invariant mass distribution similar to [4]. The corrections described in text have been applied here. Bottom figure shows data with all backgrounds (except the diboson contribution) subtracted.

6. – Conclusion

We presented in this note the invariant mass spectrum of two jets produced together with a W boson at CDF. Since the last CDF publication on this topic [4], a number of systematic effects were investigated. The most important, affecting the jet energy scale and the multijet background, resulted in large corrections that need to be applied to our background models. Using all data collected by CDF, we observe a good agreement between data and the Standard Model predictions.

REFERENCES

[1] Hagiwara K. *et al.*, *Nucl. Phys. B*, **282** (1987) 253.
[2] Kober M., Koch B. and Bleicher M., *Phys. Rev. D*, **76** (2007) 125001.
[3] Eichten E. J., Lane K. and Martin A., *Phys. Rev. Lett.*, **106** (2011) 251803.
[4] Aaltonen T. *et al.*, *Phys. Rev. Lett.*, **106** (2011) 171801.
[5] Abulencia A. *et al.*, *Nucl. Part. Phys.*, **34** (2007) 2457.
[6] Bhatti A. *et al.*, *Nucl. Instrum. Methods A*, **566** (2006) 375.
[7] Sjöstrand T. *et al.*, *JHEP*, **05** (2006) 026.
[8] CDF Collaboration, `http://www-cdf.fnal.gov/physics/new/hdg/Results_files/results/w2jet_130222/DijetMassSpectra.pdf`.
[9] CDF Collaboration, `http://www-cdf.fnal.gov/cdfnotes/cdf10926_cdfd0_ttbarxs_conf.pdf`.